

Epidemic models with digital and manual contact tracing

Dongni Zhang¹ and Tom Britton¹

¹Department of Mathematics, Stockholm University, 106 91
Stockholm, Sweden.

November 24, 2022

Abstract

We consider the Markovian SIR epidemic model but where individuals either recover naturally or are diagnosed, the latter implying isolation and subject to being contact traced. More specifically, this paper is concerned with two types of contact tracing: the classical manual contact tracing and the more recent digital contact tracing based on individuals using a tracing app, and investigates the preventive effect of each, as well as their combined preventive effect. The initial phase of an outbreak is approximated by a (two-type) branching process relying on a large community and under the simplifying assumption that contact tracing happens without delay. The "types" in the branching process are not individuals but rather "to-be-traced components". It is shown that the fraction π of app-users for the digital contact tracing needs to be bigger than the fraction p of successfully contact traced individuals in the manual contact tracing for the same preventive effect. Further, the preventive effect of combining the two contact tracing methods is shown to be bigger than the product of each of the two preventive effects.

1 Introduction

One of the main reasons for modelling epidemics is to understand the effect of different preventive measures, such as vaccination and non-pharmaceutical interventions (NPI). During the recent Covid-19 pandemic, research about

the effect of various NPIs, including social distancing, case isolation, contact tracing, lockdown, etc., has received much attention. Some related papers (e.g., [13, 15, 22]) have been highly influential on public health policies.

This paper focuses on the preventive measure: "*contact tracing*". Contact tracing is traditionally performed by public health agency officers who interview diagnosed individuals and then call the named contacts to advise them to self-quarantine and to test, which is often referred as the *manual contact tracing*. This type of contact tracing has been successful in reducing transmission in many epidemics like Ebola [26], SARS [21], Influenza [1], and Measles [20]. However, in the present paper, we also investigate a different type of contact tracing: *digital contact tracing*. In the case of Covid-19, [14] suggested that manual contact tracing is not rapid enough to control the Covid-19 epidemic, and the new idea of developing a "*contact tracing app*" was invented: once an app-user is diagnosed, a warning message will be instantaneously sent out to all the app-users who recently have been nearby for a sufficient duration with the confirmed case. Such notified contacts are then advised to test and quarantine themselves. Several contact tracing apps have been developed and released (e.g., in the UK [14, 27], in the Netherlands [17]).

There are several papers analysing digital contact tracing (e.g., [9, 18, 19, 24]) focusing on simulation-based epidemic models, and the results of [25] are based on a combination of simulations and mean-field analysis of the related percolation problem. Several papers on digital contact tracing analysing Covid-19 (e.g., [12, 14]) are based on the mathematical model first introduced by [16] in terms of recursive equations for analyzing the timing of infectiousness and the appearance of symptoms. In particular, the results from [14] showed that the Covid-19 epidemic was unlikely to be contained only by manual tracing.

Modelling contact tracing is mathematically challenging and does not easily lend itself to being analyzed using differential equations. Our focus in this paper is on the beginning of an outbreak before a massive fraction have been infected. For this reason, we apply stochastic models, which are also suitable because the outcome of contact tracing itself is random rather than deterministic. The early phase of an epidemic without preventive measures can often be approximated by a suitable branching process (e.g., [5]) using the underlying model assumption stipulating that once an individual has been infected, it behaves (transmits) independently of its infector. When contact tracing is introduced, this independence breaks down and other methods need to be developed. However, in the last decades there has been some progress in more rigorous analyses of epidemic models with manual contact tracing, e.g., [7, 8, 23].

In [28] we considered a Markovian SIR epidemic model with manual contact tracing by assuming that once individuals are diagnosed, they perform manual tracing without delay, thus reaching each contact with probability p . The model was analyzed by means of a branching process where the "individuals" of the branching processes corresponded to "to-be-traced" components, which grew and decreased over time until they eventually disappeared.

In the present paper, we first analyse a similar model as in [28] but now with digital contact tracing by assuming that a fraction π of individuals installs a contact tracing app (and follows the advice if notified). Once an app-user is diagnosed, all its app-using contacts are notified, with the result that they isolate and test themselves without delay. For those who test positive, their app-using contacts are also notified, and so on. Furthermore, for both manual and digital contact tracing, we assume that traced individuals who have recovered naturally are also identified and are subject to contact tracing.

Using large population approximations, we approximate the early epidemic process with digital tracing by a two-type branching process where type-1 "individuals" are *app-using components* (in terms of app-users) and type-2 are non-app-users. We then analyse the model having both types of contact tracing in place, i.e., reaching a fraction p of all contacts using manual contact tracing and additionally all app-using contacts if the tested individual is an app-user (making up a fraction π in the community). The limiting process in this case is shown to be a two-type branching process, where both the type-1 and type-2 "individuals" are the to-be-traced components, but type-1 starts with an app-user and type-2 with a non-app-user.

One important conclusion from the analysis is that the combined effect is better than if the two types of contact tracing act independently. More precisely, let r_M be the reduction (of the basic reproduction number) from manual contact tracing, r_D from digital contact tracing, and r_{DM} be the combined reduction. If the manual and digital tracing acts independently, then we would have $1 - r_{DM} = (1 - r_M)(1 - r_D)$, but in fact, our analysis shows that $r_{DM} > 1 - (1 - r_M)(1 - r_D)$.

In Section 2, we define the digital contact tracing model as well as the model having both manual and digital contact tracing. In Section 3, we present and prove the main result approximating the initial phase of the epidemic in a large population (Section 3.1 for digital tracing only, Section 3.2 for both types of tracing). Then, in Section 4 we illustrate our results numerically, compare the effect of manual and digital contact tracing and investigate their combined effect. Finally, we summarize our conclusions and discuss potential improvements of the present models in Section 5.

2 Epidemic models with contact tracing

2.1 The epidemic model

First, we consider a Markovian SIR (**S**usceptible \rightarrow **I**nfectious \rightarrow **R**ecovered) epidemic spreading in a closed and homogeneous mixing population with fixed size n . Initially, there is one infectious individual, and the rest are susceptible. An infectious individual has infectious contacts with each susceptible individual randomly in time according to independent Poisson processes with rate β/n , so β is the overall rate of contacts. Only contacts with susceptibles result in infection. An infectious individual recovers naturally at rate γ .

Additionally, we assume that infectious individuals are tested positive and are immediately isolated (we refer to this as "diagnosed" in our paper) at rate δ . In conclusion, infectious individuals could stop spreading disease either from natural recovery (rate γ) or diagnosis (rate δ). The infectious periods are assumed to be independent of each other and the Poisson processes.

For this epidemic model (with testing but without contact tracing), each infectious period follows the exponential distribution with intensity $(\gamma + \delta)$. Hence, it is straightforward to compute the mean number of secondary infections produced by one single infective before recovery or diagnosis:

$$R_0 = \frac{\beta}{\gamma + \delta}. \quad (1)$$

Somewhat incorrectly, we refer to this as our *basic reproduction number* R_0 in this paper, even though R_0 equals β/γ when there is no testing.

2.2 The epidemic model with digital contact tracing

We add digital contact tracing to the epidemic model in Section 2.1 by assuming that a fraction π of individuals use the tracing app (and follow the recommendations), and that individuals mix uniformly irrespective of using the app or not.

Once an infectious app-user is diagnosed, all app-using contacts of the infective will be notified, with the result that they test and isolate themselves without delay if infectious. The contacts who have been infected, including also those who have recovered, are then also assumed to trigger digital tracing among their contacts according to the same procedure, and so on.

2.3 The epidemic model with digital and manual contact tracing

Finally, we describe the epidemic model with both types of contact tracing and call this the *combined model*. First, a community fraction π are app-users and follow the instructions. If such an app-user is diagnosed, then all of its app-using contacts (on average being a fraction π of all contacts) will be traced. To this, we now add the manual contact tracing [28] by assuming that once an infectious individual is diagnosed, app-user or not, each of its contacts will be reached by manual tracing independently with probability p . It means that for diagnosed app-users, *all* app-using contacts will be traced, and each non-app-using contact will be traced with probability p . For diagnosed non-app-users, each contact, app-user or not, will be traced with probability p . Like before, all traced individuals are tested and isolated without delay if testing positive. Traced individuals who test positive, including also those who have recovered, are then contact traced in the same manner without delay, and so on.

In the case of $\pi = 0$, this model corresponds to our earlier model with manual tracing only in [28], and if $p = 0$ it corresponds to the model with digital tracing only in Section 2.2. The model parameters are summarized in Table 2.1.

Table 2.1 Table of Model Parameters

Parameter	Notation
size of population	n
transmission rate	β
rate of natural recovery	γ
rate of diagnosis	δ
community fraction using the contact tracing app (and following the advice)	π
probability that contact is manually traced successfully or naturally recovered contact manually	p

3 Approximation of the initial phase in a large community

When the population size n is large, it is very unlikely that infectious contacts will be with already infected people. In fact, the first contact with someone who has already been infected will happen when around \sqrt{n} individuals have been infected (see, e.g., [2] page 25). Consequently, at the beginning of the epidemic in a large community, individuals will infect approximately independently of each other while infectious, which can be made precise using coupling methods (see [5]). However, also in the limit as $n \rightarrow \infty$ infectious individuals will *not* behave completely independently since an infectious individual may be contact traced by its infector or one of its infectees.

As a consequence, when contact tracing is introduced, the limiting process of infectious individuals will *not* be a branching process as is usually the case for epidemic models. For this reason, we consider "to-be-traced" components as "macro-individuals" since these components will behave independently between generations. In the following sections, we first describe the limiting branching processes for the model with digital tracing and then for the combined model.

3.1 The epidemic model with digital contact tracing

When digital tracing is in place, the population comprises app-users and non-app-users. A given infectious app-user has the possibility of being traced and hence stops being infectious when one of its app-using contacts is diagnosed. It implies that infectious app-users no longer infect independently of each other in our model.

Instead of describing the limiting process in terms of the actual individuals, we consider to-be-traced components as "macro-individuals": since contact tracing will never happen between such components, these components behave independently of each other and may hence be approximated by a branching process (see [28]). Here we focus on the so-called *app-using components* (to-be-traced components in terms of app-users). Such app-using components will start with one infectious app-user infected by a non-app user (we call this the *root* of the component) but can later grow to include the app-users infected by the root and app-users they infected, and so on. Eventually, the whole app-using component will die out (i.e., stop spreading the infection) either by someone being diagnosed (when immediately the whole component gets traced and diagnosed) or if all individuals in the component have recovered naturally. While the component has infectious individuals,

the component can also infect non-app-users. Non-app-users can, in turn, infect other non-app-users as well as app-users, and in the latter case, new app-using components are created.

In Figure 3.1, we show how the two types of "individuals": app-using components (surrounded by dashed lines) and non-app-users (square-shaped nodes) grow and eventually die out. We set the app-user $A1$ to be the initial case. While the app-using component $C_1^{(app)}$ evolves (new app-users getting infected or existing ones recovering), the component $C_1^{(app)}$ infects two non-app-users $N1$ and $N2$. The non-app-user $N1$ infects one non-app-user and one new app-using component $C_2^{(app)}$ with root $A2$, whereas $N2$ infects two other non-app-users. Once the app-user $A2$ is diagnosed, the whole app-using component $C_2^{(app)}$ will die out.

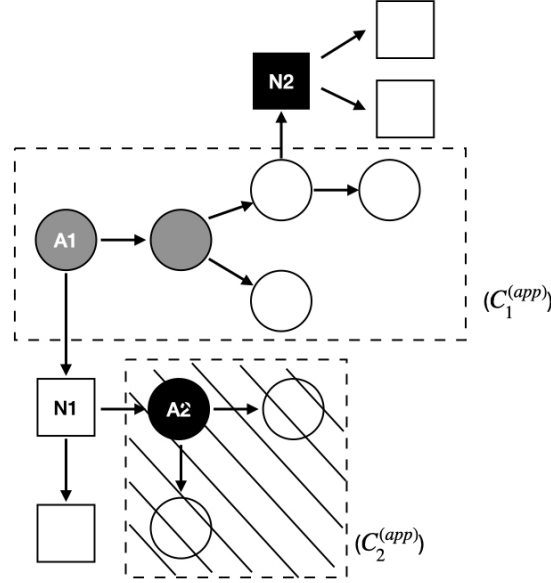


Figure 3.1 Example of the dynamics of app-using components and non-app-users for the model with digital contact tracing: the circle nodes are app-users and the squares non-app-users. The white, black, and grey nodes are regarded as "infectious", "diagnosed" and "naturally recovered", respectively. The rectangular region surrounded by the dashed line symbolizes the app-using component, and the area is filled with diagonal lines when the whole component is diagnosed and removed.

In conclusion, we consider a two-type branching process $E_D(\beta, \gamma, \delta, \pi)$ with the type-1 individuals being app-using components and the type-2 being non-app-users, where a new birth corresponds to a new infection in the epidemic. Then with the *coupling* argument (see [2, 5, 11]), it can be easily

proved that the epidemic process in terms of the app-using components and non-app-users converges to this two-type branching process for large n .

3.1.1 Properties of the limiting branching process

We have seen that during the early stage of an outbreak and in the large population, the epidemic process with digital tracing can be approximated by the two-type branching process $E_D(\beta, \gamma, \delta, \pi)$.

In this section, we derive the component reproduction number R_D for the model with digital tracing as the largest eigenvalue of the mean offspring matrix M of $E_D(\beta, \gamma, \delta, \pi)$ (see e.g., [3, 10]) with

$$M = \begin{pmatrix} m_{11} & m_{12} \\ m_{21} & m_{22} \end{pmatrix}, \quad (2)$$

where m_{ij} is the number of secondary infections of type j produced by a single infected individual of type i on average, for $i, j = 1, 2$. And hence the component reproduction number R_D is given by

$$R_D = \frac{m_{11} + m_{22}}{2} + \sqrt{\frac{(m_{11} + m_{22})^2}{4} - m_{11}m_{22} + m_{12}m_{21}}. \quad (3)$$

Next, we derive the expressions for the elements m_{ij} as follows. We note that the dynamics of app-using components (type 1) works similarly to the "to-be-reported components" studied in [28], *except* that here an app-using component can not infect a new component, because infected app-users will belong to the same component. Consequently, we have that

$$m_{11} = 0. \quad (4)$$

The group of non-app-users will never be reached by digital tracing and thus spread the infection simply like in a general epidemic without any contact tracing. That is, each infectious non-app-user infects non-app-users at rate $\beta(1 - \pi)$ and app-users at rate $\beta\pi$, where the infectious periods of non-app-users are independent and identically exponentially distributed with intensity $(\delta + \gamma)$. Hence, the number of app-using component (type 1) and non-app-users (type 2) infected by one typical non-app-user are *geometrically* distributed with mean

$$m_{21} = \frac{\beta\pi}{\delta + \gamma}, \quad (5)$$

and

$$m_{22} = \frac{\beta(1 - \pi)}{\delta + \gamma} \quad (6)$$

respectively.

Finally, it remains to compute m_{12} . Following the idea in [28], let $Z^{(a)}$ be the total number of non-app-users born by an app-using component, then we have

$$m_{12} = \mathbb{E}[Z^{(a)}] = \mathbb{E}\left[\sum_{i=1}^{N_c^{(a)}} X_i^{(na)}\right],$$

where $X_i^{(na)}$ denotes the number of non-app-users infected between the $i-1$ 'th and the i 'th jump, and $N_c^{(a)}$ denotes the number of jumps that an app-using component makes before dying out and hence stopping infecting.

For the distribution of $X_i^{(na)}$ and $N_c^{(a)}$, we briefly state the idea as follows (see [28] for details). If currently there are k infectious app-users in an app-using component, the size of this component increases by 1 when the component infects an app-user, hence at rate $k\beta\pi$; decreases by 1 if there is a natural recovery (rate $k\gamma$); and drops to 0 if an app-user is diagnosed which happens at rate $k\delta$. Thus we consider the process of app-using components as a simple random walk (new infection/ natural recovery) with "killing events" (diagnosis) added. $N_c^{(a)}$ is the number of jumps until the component has no infectives, something which can happen either if all infectious app-user have recovered naturally or if an infectious app-user is diagnosed.

Furthermore, if currently there are k infectives in the component, the time until the next event occurs is exponentially distributed with intensity $k(\beta\pi + \gamma + \delta)$. During this time, such component infects the non-app-users at $k\beta(1 - \pi)$. It follows that the numbers $X_i^{(na)}$ of infections of non-app-users between jumps are identically and independently distributed (geometric distributed with mean $\beta(1 - \pi)/(\beta\pi + \gamma + \delta)$) and independent of the current size of the component.

Consequently, we derive the mean number m_{12} of non-app-users (type 2) infected by an app-using component (type 1) given by

$$m_{12} = \mathbb{E}[X^{(na)}]\mathbb{E}[N_c^{(a)}], \quad (7)$$

with

$$\mathbb{E}[X^{(na)}] = \frac{\beta(1 - \pi)}{\beta\pi + \gamma + \delta}, \quad (8)$$

and

$$\mathbb{E}[N_c^{(a)}] = 1 + \sum_{k=1}^{\infty} \mathbf{P}(N_c^{(a)} > k), \quad (9)$$

where for $k \geq 1$, the distribution of $N_c^{(a)}$ is given by

$$\mathbf{P}(N_c^{(a)} > k) = \left(1 - \sum_{j=1}^{\lceil k/2 \rceil} \frac{1}{2j-1} \binom{2j-1}{j} \left(\frac{\beta\pi}{\gamma + \beta\pi}\right)^{j-1} \left(\frac{\gamma}{\gamma + \beta\pi}\right)^j\right) \cdot \left(\frac{\beta\pi + \gamma}{\beta\pi + \gamma + \delta}\right)^k.$$

In conclusion, we obtain with Equation (3) that the component reproduction number R_D for the model with digital tracing only is given by

$$R_D = \frac{m_{22}}{2} + \sqrt{\frac{m_{22}^2}{4} + m_{12}m_{21}}, \quad (10)$$

with the elements m_{ij} given by Equations (5)-(7). Using the theory of branching processes (see e.g. [2, 4]), we collect our findings in the following proposition:

Proposition 3.1. *Consider a sequence of epidemic processes with digital tracing $E_D^{(n)}(\beta, \gamma, \delta, \pi)$, for population size n , and starting with one initial infective. Then on any finite time interval, $E_D^{(n)}(\beta, \gamma, \delta, \pi)$ converges in distribution to the two-type branching process $E_D(\beta, \gamma, \delta, \pi)$ as $n \rightarrow \infty$.*

Let Z_∞ denote the number of individuals ever born in the branching process $E_D(\beta, \gamma, \delta, \pi)$, then we have $\mathbf{P}(Z_\infty < \infty) = 1$ if $R_D \leq 1$ and $\mathbf{P}(Z_\infty < \infty) < 1$ if $R_D > 1$.

Let Z_n be the final number infected in the epidemic, then $\mathbf{P}(Z_n > \sqrt{n}) \rightarrow 0$ as $n \rightarrow \infty$ if and only if $R_D \leq 1$.

3.1.2 The individual reproduction number

The interpretation of R_D is complicated in that the two types in the underlying branching process $E_D(\beta, \gamma, \delta, \pi)$ are different types of objects: type-2 individuals are actual individuals (non-app-users), but type-1 are "macro individuals": the to-be-traced app-using components. In this section, our aim is to convert R_D to an individual reproduction number.

We first define the average number of individuals (of any type) $R_{D-A}^{(ind)}$ infected by a newly infected app-user and $R_{D-N}^{(ind)}$ by a non-app-user, respectively. We note that each infection, irrespective of the type of infector, is with an app-user with probability π and a non-app-user with probability $(1 - \pi)$. This implies that the $R_D^{(ind)}$ can be expressed as the sum:

$$R_D^{(ind)} = \pi R_{D-A}^{(ind)} + (1 - \pi) R_{D-N}^{(ind)}. \quad (11)$$

It remains to compute the $R_{D-A}^{(ind)}$ and $R_{D-N}^{(ind)}$. From the previous results in Section 3.1.1, we see that a given app-using component infects on average

m_{12} number of non-app-users. Let $\mu_c^{(A)}$ be the mean number of app-users that ever get infected in an app-using component. All but one of these $\mu_c^{(A)}$ are infected within the component, and there are, on average, m_{12} number of "external" infections. So in total, there are on average $(\mu_c^{(A)} - 1) + m_{12}$ number of infections by an app-using component. As a consequence, the average number $R_{D-A}^{(ind)}$ of infections *per app-user* equals

$$R_{D-A}^{(ind)} = \frac{(\mu_c^{(A)} - 1) + m_{12}}{\mu_c^{(A)}}, \quad (12)$$

where

$$\mu_c^{(A)} = 1 + \frac{\beta\pi}{\beta\pi + \gamma} \sum_{k=1}^{\infty} \mathbf{P}(N_c^{(a)} > k - 1) = 1 + \frac{\beta\pi}{\beta\pi + \gamma} \mathbb{E}[N_c^{(a)}]. \quad (13)$$

We skip the proof for the computation of $\mu_c^{(A)}$; an identical argument was used in [28].

For non-app-users, it is easier to analyse since a given infectious non-app-user, on average, infects $m_{21} + m_{22}$ number of individuals (app-users and non-app-users). Using Equations (5) and (6) it follows that

$$R_{D-N}^{(ind)} = m_{21} + m_{22} = \frac{\beta}{\delta + \gamma}, \quad (14)$$

which is identical to R_0 (see Equation (1)). This is not surprising since non-app-users will never be contact traced.

An individual reproduction number $R_D^{(ind)}$ for digital tracing is thus given by

$$R_D^{(ind)} = \pi \frac{(\mu_c^{(A)} - 1) + m_{12}}{\mu_c^{(A)}} + (1 - \pi) \frac{\beta}{\delta + \gamma}, \quad (15)$$

with m_{12} defined in Equation (7) and $\mu_c^{(A)}$ in Equation (13).

Remark 3.1. *As discussed in [28], this individual reproduction number $R_D^{(ind)}$ does not possess the traditional interpretation: the average number of infections caused by infected people at the beginning of the outbreak. This is due to the delicate timing of event issues closely related to those explained in [6]. However, it still has the correct threshold property as supported numerically in Section 4.*

3.2 The epidemic model with digital and manual contact tracing

We now analyse the combined model with both manual and digital contact tracing.

3.2.1 Properties of limiting branching process

Also, the combined model can be approximated by a suitable two-type branching process $E_{DM}(\beta, \gamma, \delta, p, \pi)$ during the early stage of the epidemic, assuming a large population. Clearly, for the combined model, the app-users could not only be traced by app-users, but also by non-app-users with probability p . On the other hand, the non-app-users could be traced by individuals (either app-users or non-app-users) with probability p . Accordingly, to-be-traced components now make up infections between app-users and non-app-users who will be traced manually. Moreover, new components are created if an app-user infects a non-app-user without manual contact tracing taking place or if a non-app user infects either type and there is no manual contact tracing. The new components hence differ in how they are created: with an app-user (infected by a non-app-user without manual contact tracing) or a non-app-user (without manual contact tracing), and the future evolvement of such components depend on the current number of infectious app-users and non-app-users. We hence have two types of to-be-traced components, depending on if it was initiated by an app-user or non-app-user. A component starting with a non-app-user increases its size at rate βp (only manual tracing works for non-app-users), whereas a component starting with an app-user increases its size at rate $\beta(1 - \pi)p + \beta\pi$.

Next, we give an example in Figure 3.2 to illustrate how the two types of components (starting with an app-user or a non-app-user) grow and reproduce. We start with case 1, which is the root of the component $C_1^{(NA)}$, which generates two new components $C_2^{(NA)}$ and $C_3^{(A)}$. The component $C_2^{(NA)}$ is with root 2 as a non-app-user and $C_3^{(A)}$ starts with an app-user 3. Once individual 1 is diagnosed, the whole component $C_1^{(NA)}$ is diagnosed.

Another difference from the analysis for digital tracing is that the to-be-traced components may also contain non-app-users that are manually traced. So it is necessary to keep track of both the number of infectious app-users and infectious non-app-users in the component.

Let $N_j^{(i)}(t)$ be the number of infectious type- j individuals in the component starting with one type- i individual at time t , where we set type-1 to be

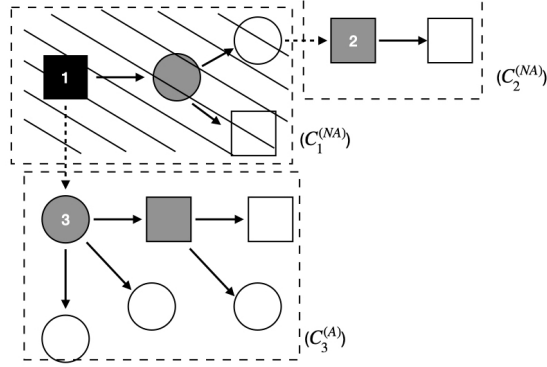


Figure 3.2 Example of the process of to-be-traced components started by app-users and non-app-users for the combined model: the circles are app-users and squares non-app-users. The nodes in white, black, and grey are regarded as "infectious", "diagnosed" and "naturally recovered", respectively. The rectangular region surrounded by the dashed line is for the component, whereas the area is filled with slashed lines when the whole component is removed. Full edges stand for contacts that could be traced either by manual or digital contact tracing (so always full edges between each pair of app-users), whereas dashed ones are for those non-to-be-traced.

app-users and type-2 to be non-app-users. Suppose that at time t we have

$$N^{(i)}(t) = (k, l), \text{ i.e. } = (N_1^{(i)}(t) = k, N_2^{(i)}(t) = l),$$

i.e. there are k infectious app-users and l infectious non-app-users in a component starting with a type- i individual. We note that $N^{(1)}(0) = (1, 0)$, whereas $N^{(2)}(0) = (0, 1)$.

$N^{(i)}$ increases or decreases by 1 in the first component if there is a newly infected app-user or one of the k app-users recovers naturally, respectively. The rate at which $N^{(i)}$ increases by $(1, 0)$ is hence $k\beta\pi + l\beta\pi p$ (the rate that app-users infect plus the rate at which non-app-users infect), and $N^{(i)}$ decreases by $(-1, 0)$ at rate $k\gamma$ (recovery of an app-user). Further, $N^{(i)}$ increases by 1 in the second component at rate $(k + l)\beta(1 - \pi)p$, because this newly infected non-app-user shall have a manual tracing link, irrespective of the type of infector. Furthermore, $N^{(i)}$ decreases by 1 in the second component at rate $l\gamma$ (recovery of a non-app-user). Finally, $N^{(i)}$ drops directly to $(0, 0)$ at rate $(k + l)\delta$ when one of the infectious individuals (of either type) in the component is diagnosed.

Next, we describe the birth of new components. We note that only infections with no digital or manual contact tracing links create a new component.

This can only occur to pairs of non-app-users or pairs of app-users and non-app-users, but it never happens between two app-users. As a consequence, given that there are $N^{(i)}(t) = (k, l)$ (k infectious app-users and l infectious non-app-users), the component gives birth to new components with an app-using root at rate $l\beta\pi(1-p)$, and new components with a non-app-using root at rate $(k+l)\beta(1-\pi)(1-p)$.

In conclusion, at the beginning of an outbreak and for a large population, we approximate the epidemic with both manual and digital tracing by a two-type branching process $E_{DM}(\beta, \gamma, \delta, p, \pi)$ with "individuals" of type 1 are to-be-traced components starting with an app-user and type 2 "individuals" are components with a non-app-using root. Again, we can apply the *coupling* argument (see, e.g., [2, 5, 11]) to show that the epidemic process in terms of the two type components converges to the two-type branching process $E_{DM}(\beta, \gamma, \delta, p, \pi)$ as $n \rightarrow \infty$.

Now we derive the corresponding component reproduction number R_{DM} which is known as the dominant eigenvalue of the corresponding mean offspring matrix $M^{(c)}$ (see [3, 10]) given by :

$$M^{(c)} = \begin{pmatrix} m_{11}^{(c)} & m_{12}^{(c)} \\ m_{21}^{(c)} & m_{22}^{(c)} \end{pmatrix}, \quad (16)$$

in which the element $m_{ij}^{(c)}$, is the mean number of new components of type j produced by a single component of type i , for $i, j = 1, 2$. The component reproduction number R_{DM} is hence given by

$$R_{DM} = \frac{m_{11}^{(c)} + m_{22}^{(c)}}{2} + \sqrt{\frac{(m_{11}^{(c)} + m_{22}^{(c)})^2}{4} - m_{11}^{(c)}m_{22}^{(c)} + m_{12}^{(c)}m_{21}^{(c)}}. \quad (17)$$

Based on the previous discussion, we have derived the birth rates of new components of type i conditional on $N^{(i)}(t)$. The expected total numbers $m_{ij}^{(c)}$ of new type- j components produced by a type- i component are hence the expected values of these expressions integrated over time:

$$m_{11}^{(c)} = \int_0^\infty \mathbb{E}[N_2^{(1)}(t)]\beta\pi(1-p)dt, \quad (18)$$

$$m_{12}^{(c)} = \int_0^\infty (\mathbb{E}[N_1^{(1)}(t)] + \mathbb{E}[N_2^{(1)}(t)])\beta(1-\pi)(1-p)dt, \quad (19)$$

$$m_{21}^{(c)} = \int_0^\infty \mathbb{E}[N_2^{(2)}(t)]\beta\pi(1-p)dt, \quad (20)$$

$$m_{22}^{(c)} = \int_0^\infty (\mathbb{E}[N_1^{(2)}(t)] + \mathbb{E}[N_2^{(2)}(t)])\beta(1-\pi)(1-p)dt. \quad (21)$$

We have not been able to simplify these expressions further analytically. The main reason for this is that *not* all the rates of the four events occurring in the component are linear in the number of infectious individuals. In particular, the rate at which $N^{(i)} = (k, l)$ increases in the first component equals $k\beta\pi + l\beta\pi p$ (non-linear in $k + l$).

In Section 4, we perform simulations to derive the m_{ij} and numerically compute the component reproduction number R_{DM} for given parameters. Based on the numerical results, we analyze how R_{DM} depends on the manual tracing probability p and the app-using fraction π .

3.2.2 The reduction effect of manual and digital contact tracing

We recall that $R_0 = \beta/(\delta + \gamma)$ is the basic reproduction number (without any type of contact tracing), R_M is the effective component reproduction number for manual tracing only (derived in [28]), R_D is the component reproduction number for digital tracing only (Equation (3)), and R_{DM} is the component reproduction number for the combined model (Equation (17)).

Further, let r_M, r_D and r_{DM} denote the three relative reductions (of R_0) by manual, digital contact tracing only and both type of contact tracing, respectively:

$$R_M = (1 - r_M)R_0, R_D = (1 - r_D)R_0, R_{DM} = (1 - r_{DM})R_0.$$

If the two effects from manual and digital contact tracing acted independently when combined, we would have

$$1 - r_{DM} = (1 - r_M)(1 - r_D),$$

which implies that the reproduction number for the combined model would be given by

$$(1 - r_M)(1 - r_D)R_0. \tag{22}$$

Remark 3.2. *It is worth highlighting that the reproduction numbers R_0, R_D, R_M and R_{DM} are not in the same scale, however all of them are epidemic thresholds meaning that the models are super-critical if and only if the corresponding reproduction number exceeds 1. For this reason, we mainly focus on the cases when the quantity in Equation (22) equals one: if we have $R_{DM} < 1$ and $R_0(1 - r_M)(1 - r_D) > 1$, then the combined effect (of reducing R_0) would be bigger than the product of each of the preventive effects.*

Later in Section 4, we will plot the critical combinations of (p, π) for which R_{DM} equals 1 and the corresponding values for which $(1 - r_M)(1 - r_D)R_0$ equals 1. And it will show that the reduction r_{DM} is in fact bigger than $1 - (1 - r_M)(1 - r_D)$.

4 Numerical Illustration

In this section, we numerically compare the effects of digital and manual tracing and the combined model. We also investigate the effect of the testing rate δ , where we vary the fraction getting tested: $\delta/(\delta+\gamma)$ rather than varying δ . For all the numerical results below (except Table 4.1), we set the epidemic parameters to be fixed: $\beta = 6/7, \gamma = 1/7$ so that the reproduction number without any testing or contact tracing is $\beta/\gamma = 6$. When also considering diagnosis ($\delta > 0$), we would have the basic reproduction number $R_0 = \beta/(\gamma + \delta)$ smaller than 6.

4.1 Comparison of digital and manual tracing only

In Figure 4.1a, we plot the necessary testing rate (measured by testing level $(\delta/(\delta+\gamma))$) for which the manual R_M equals 1 (see [28]) and digital component reproduction number R_D equals 1 (see Equation (10)), for a given value of p and π respectively. It shows that for a given testing level $\delta/(\delta + \gamma)$, a larger app-using fraction π is required compared to p , the fraction of contacts that are successfully manually traced, for which the corresponding reproduction number equals 1. The explanation is that the effectiveness of digital contact tracing is more connected to the square of the fraction of app-users (π^2): the digital tracing is carried out only if both the confirmed case and the contact are app-users.

In Figure 4.1b, we hence plot the critical combination of $\delta/(\delta + \gamma)$ against π^2 instead. It can be seen that the curve for π^2 is closer to the one for p , but still not identical: we still need a larger value on π^2 for the reproduction number to equal unity.

4.2 The individual and component reproduction numbers for digital tracing only

In Figure 4.2, we plot how the digital reproduction number R_D and individual reproduction number $R_D^{(ind)}$ vary with the testing fraction $\delta/(\delta + \gamma)$ in $[0, 5/6]$ and the fraction of app-users π in $[0, 1]$. By looking at the colors at the bottom in Figure 4.2a, we observe that the component reproduction number R_D is *not* monotonically decreasing in π , the fraction of app-users. This is a highly surprising result since we expect a smaller reproduction number for a bigger fraction π that use the app and hence perform digital contact tracing.

This non-monotonicity of R_D is explained as follows. First of all, it can be easily seen from Equations (5) and (6) that the element m_{21} is increasing and m_{22} is decreasing with π . Then, at a very low level of testing fraction,

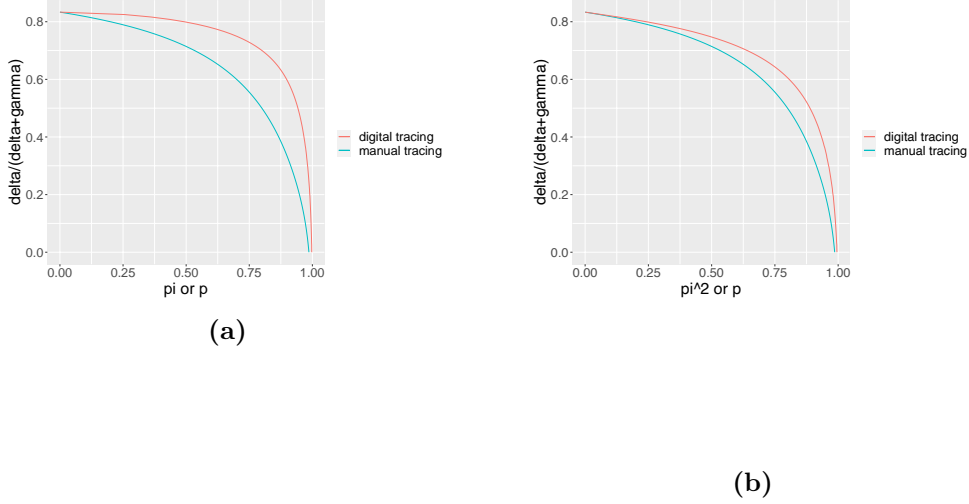


Figure 4.1 Plot of the effective combination of testing fraction $\delta/(\delta + \gamma)$ and tracing probability (manual tracing probability p or 4.1a: fraction π of app-users; 4.1b: squared fraction π^2 of app-users) such that the reproduction number (R_M or R_D) equals one: the curve (in red) is for model only with digital tracing, whereas the curve (in blue) is for model only with manual tracing.

increasing π leads to more app-users, and thus the *size* of the app-using component will grow even if fewer non-app-users will be infected per app-user. The average number of non-app-users infected by one app-using component m_{12} may hence increase with π . Then according to the expression of R_D (see Equation (10)), R_D could increase with π when the testing fraction $\delta/(\delta + \gamma)$ is low. On the other hand, we see from Figure 4.2b that the individual reproduction number $R_D^{(ind)}$ is monotonically decreasing in π as expected.

Further, we check if the individual reproduction number $R_D^{(ind)}$ has the correct threshold property, i.e. see if it equals 1 exactly when R_D does. We first fix the testing rate $\delta = 1/7$, so that there are 50% of the infected individuals are tested and isolated, and 50% recover naturally while still infectious, implying that $R_0 = \beta/(\gamma + \delta) = 3$. Then we compare the app-using fractions π such that $R_D^{(ind)}$ or R_D equals 1. In Figure 4.3, we plot the curves of reproduction numbers $R_D^{(ind)}$ (in red) and R_D (in blue) against the fraction of app-users π , where it seems to confirm that both reproduction numbers equal 1 at the same π , thus supporting our conjecture in Remark

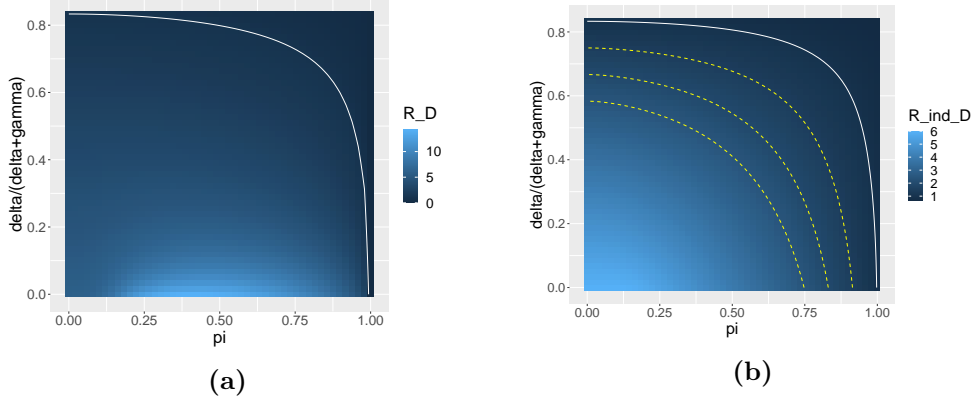


Figure 4.2 Heatmap of the effective reproduction number, 4.2a for component reproduction number and 4.2b for individual reproduction number varying with testing fraction $\delta/(\delta + \gamma)$ and fraction of app-users π ; with $\beta = 6/7, \gamma = 1/7$ fixed. The lines indicate where $R_D = 1$ (in white) and $R_D^{(ind)} = 2.5, 2, 1.5$ (in yellow dashed, from left to right) and 1 (in white), respectively.

(3.1).

4.3 Effect of combination of digital and manual tracing

Finally, we perform simulations to derive the reproduction number R_{DM} for the combined model shown in Figure 4.4. In Figure 4.4a, we show the heatmap of R_{DM} as a function of p and π (for $\delta = 1/7$) and add two curves: one curve is the true reproduction number $R_{DM} = 1$ in Equation (17) and the second curve is the naïve guess one $R_0(1 - r_D)(1 - r_M) = 1$ in Equation (22).

We see from Figure 4.4a that the reproduction number R_{DM} appears to be monotonically decreasing both with fraction p of being successfully manually contact traced and the fraction π of app-users. Moreover, we observe from the two critical curves that for any combination of (p, π) such that the naïve guess $R_0(1 - r_D)(1 - r_M) = 1$, we have the true reproduction number $R_{DM} < 1$. It implies that the combined effect of having both manual and digital tracing is bigger than the product of the preventive effect when having each one of them. An explanation to this is that a contact tracing event from digital contact tracing also shortens the infectious periods for some possible infections where manual tracing would take place, and vice versa.

Nevertheless, we note that for small values of $\delta/(\delta + \gamma)$, the component reproduction number R_D can be increasing in π . Similarly for the combined model, if we choose $\delta = 1/28$ (not realistic but as an illustration), we see in

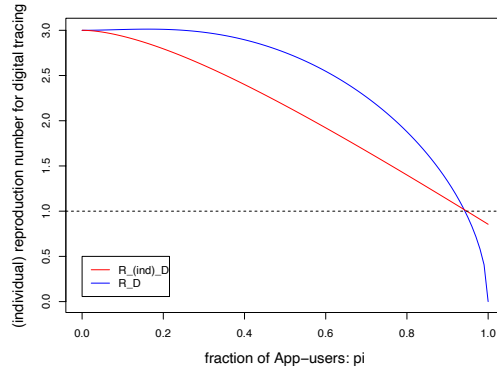


Figure 4.3 Plot of two curves of $R_D^{(ind)}$ (in red) and R_D (in blue) against π with $\beta = 6/7, \gamma = 1/7$ and $\delta = 1/7$ fixed. The horizontal dashed line stands for when the reproduction number equals 1.

Figure 4.4b that the component reproduction number R_{DM} is *not* monotonically decreasing with either probability p or π . And the curve of $R_{DM} = 1$ seems to be monotonically decreasing.

Finally in Table 4.1, we compute the reproduction number R_{DM} and its naïve guess $R_0(1 - r_D)(1 - r_M)$ in four different cases: without any contact tracing ($p = \pi = 0$); with digital tracing only ($p = 0, \pi = 2/3$); with manual tracing only: ($p = 2/3, \pi = 0$) and with both manual and digital tracing ($p = \pi = 2/3$), keeping all other parameters fixed: $\beta = 0.8, \gamma = 1/7, \delta = 1/7$. For each case, we perform 10 000 simulations of the epidemic with the chosen parameters and population size $n = 5000$, starting with one initial infective. It can be seen from Table 4.1 that the fraction of major outbreaks (considered as more than 10% have been infected) and the mean fraction of infected among the major outbreaks both *decrease* with the reproduction number, as expected (see Proposition 3.1).

In particular, from the last line of Table 4.1 we note that R_{DM} is below 1 even if the naïve guess $R_0(1 - r_D)(1 - r_M)$ is above 1, which confirms that

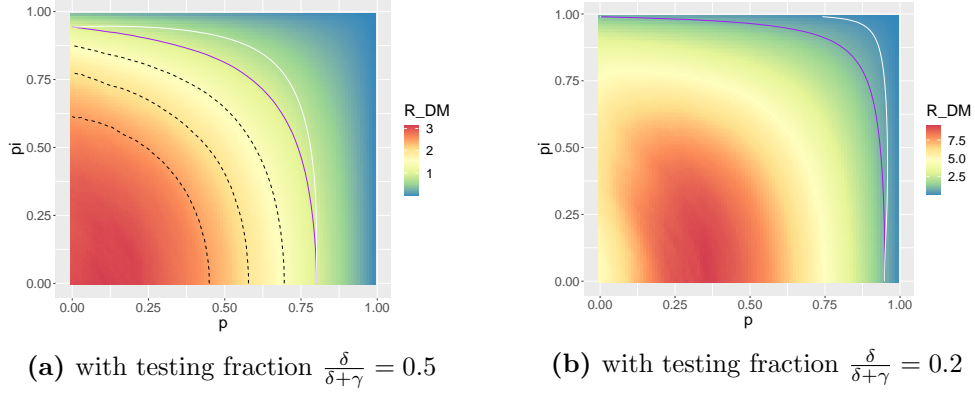


Figure 4.4 Plot of reproduction number R_{DM} for the combined model varying with manual tracing probability p and fraction of app-users π ; with $\beta = 6/7, \gamma = 1/7$ fixed, 4.4a for $\delta = 1/7$ and 4.4b for smaller $\delta = 1/28$: the curve in purple stands for the case when $R_{DM} = 1$ and the curve in white for the case when $R_0(1 - r_D)(1 - r_M) = 1$. Moreover, the dashed lines in black in 4.4a are for the cases when $R_{DM} = 2.5, 2, 1.5$, respectively from left to right.

the combined effect of both manual and digital tracing is bigger than two separate effects multiplied by each other, i.e. $r_{DM} > 1 - (1 - r_D)(1 - r_M)$.

Table 4.1 Simulation results in four different cases of p and π

p	π	the reproduction number	fraction of major outbreaks	mean fraction of infected among major outbreaks
0	0	$R_0 = 2.80$	0.64	0.93
0	2/3	$R_D = 2.20$	0.49	0.81
2/3	0	$R_M = 1.49$	0.46	0.75
2/3	2/3	$R_{DM} = 0.92$	0.01	0.14
		$R_0(1 - r_D)(1 - r_M) = 1.17$		

5 Discussion

In this paper, we analyzed a Markovian epidemic model with digital as well as manual contact tracing. For the epidemic model with digital tracing only, the early stage of the epidemic was approximated by a two-type branching process with one type being to-be-traced app-using components and the other being non-app-users, and R_D being the largest eigenvalue of the matrix of mean offspring. The individual reproduction number $R_D^{(ind)}$ was also derived.

The dependency of reproduction numbers on the effectiveness of testing and contact tracing was assessed analytically and numerically. Surprisingly, the reproduction number R_D for digital tracing was not monotonically decreasing in π , the fraction of app-users, whereas the individual reproduction number $R_D^{(ind)}$ seems to be. When comparing digital tracing with manual tracing, a smaller tracing probability p is needed than the corresponding app-using fraction π to reach the same effectiveness. This result is not very surprising because both sides of the infection need to be app-users for digital contact tracing to take place.

We then analyzed the combined model and approximated the beginning of the epidemic by a different two-type branching process, with both types being to-be-traced components and only differing on the type of the root (app-user or not). The corresponding reproduction number was derived numerically. Importantly, the preventive effect of combining the two contact tracing methods was shown to be bigger than the product of two separate effects.

There are several extensions of the present model that would make it more realistic. On the one hand, we assume that there is no delay in both manual and digital contact tracing, i.e., any traced contact (either by manual or digital tracing) is assumed to be immediately diagnosed. This neglects one crucial difference between manual and digital tracing: manual tracing is time- and labor-intensive, so there is often a delay between the case confirmation and notification of contacts, whereas digital tracing is designed to avoid (or shorten) the delay. Additionally, one limitation of a contact tracing app is that there could be close contacts that can lead to transmission but occur too quickly to be recorded by the app. In this sense, our model could be extended by considering the fact that not all the contacts between pairs of app-users could be reached by digital tracing. Further, we make the simplifying assumption that traced individuals who have by then recovered are also identified and contact traced (see [23] which do not make this assumption). In reality, this may happen for individuals who have recently recovered, but perhaps not for those who have recovered several weeks earlier. Therefore, our results in this paper give an upper bound on how effective the real contact tracing would be.

A different extension would be to consider a structured community (e.g., a social network) combined with homogeneous random contacts. Then, digital contact tracing would work in the same way for random contacts and contacts in the social network (as long as both are app-users), whereas manual contact tracing would most likely only happen on the social network (very rarely could you name whom you sat next to in the bus).

On the mathematical side, we only focus on the early stage of the epidemic

in this paper. Analysing later parts of the epidemic remains open. Moreover, there are problems with obtaining an analytic expression for the reproduction number for the combined model.

Despite these model limitations, we consider our contribution an important step in increasing understanding of the effect of different contact tracing forms on spreading disease.

Acknowledgments

T.B. is grateful to the Swedish Research Council (grant 2020-04744) for financial support.

References

- [1] Manju Agarwal and Archana S. Bhadauria, *Modeling H1N1 flu epidemic with contact tracing and quarantine*, International Journal of Biomathematics **05** (2012), no. 05, 1250038.
- [2] Håkan Andersson and Tom Britton, *Stochastic Epidemic Models and Their Statistical Analysis* (P. Bickel, P. Diggle, S. Fienberg, K. Krickeberg, I. Olkin, N. Wermuth, and S. Zeger, eds.), Lecture Notes in Statistics, vol. 151, Springer New York, New York, NY, 2000.
- [3] Krishna B. Athreya and Peter E. Ney, *Branching Processes*, Springer Berlin Heidelberg, Berlin, Heidelberg, 1972.
- [4] Frank Ball and Damian Clancy, *The final outcome of an epidemic model with several different types of infective in a large population*, Journal of Applied Probability **32** (1995), no. 3, 579–590.
- [5] Frank Ball and Peter Donnelly, *Strong approximations for epidemic models*, Stochastic Processes and their Applications **55** (1995), no. 1, 1–21.
- [6] Frank Ball, Lorenzo Pellis, and Pieter Trapman, *Reproduction numbers for epidemic models with households and other social structures ii: Comparisons and implications for vaccination*, Mathematical Biosciences **274** (2016), 108–139.
- [7] Frank G. Ball, Edward S. Knock, and Philip D. O’Neill, *Threshold behaviour of emerging epidemics featuring contact tracing*, Advances in Applied Probability **43** (2011), no. 4, 1048–1065.
- [8] M. T. Barlow, *A branching process with contact tracing* (2020). Publisher: arXiv Version Number: 1.
- [9] A. Barrat, C. Cattuto, M. Kivelä, S. Lehmann, and J. Saramäki, *Effect of manual and digital contact tracing on COVID-19 outbreaks: a study on empirical contact data*, Journal of The Royal Society Interface **18** (2021), no. 178, rsif.2020.1000, 20201000.
- [10] Niels Becker and Ian Marschner, *The effect of heterogeneity on the spread of disease*, Stochastic Processes in Epidemic Theory, 1990, pp. 90–103. Series Title: Lecture Notes in Biomathematics.

- [11] Tom Britton, *Stochastic epidemic models: A survey*, Mathematical Biosciences **225** (2010), no. 1, 24–35.
- [12] G. Cencetti, G. Santin, A. Longa, E. Pigani, A. Barrat, C. Cattuto, S. Lehmann, M. Salathé, and B. Lepri, *Digital proximity tracing on empirical contact networks for pandemic control*, Nature Communications **12** (2021), no. 1, 1655.
- [13] N Ferguson, D Laydon, G Nedjati Gilani, N Imai, K Ainslie, M Baguelin, S Bhatia, A Boonyasiri, ZULMA Cucunuba Perez, G Cuomo-Dannenburg, A Dighe, I Dorigatti, H Fu, K Gaythorpe, W Green, A Hamlet, W Hinsley, L Okell, S Van Elsland, H Thompson, R Verity, E Volz, H Wang, Y Wang, P Walker, P Winskill, C Whittaker, C Donnelly, S Riley, and A Ghani, *Report 9: Impact of non-pharmaceutical interventions (NPIs) to reduce COVID19 mortality and healthcare demand*, Imperial College London, 2020.
- [14] Luca Ferretti, Chris Wymant, Michelle Kendall, Lele Zhao, Anel Nurtay, Lucie Abeler-Dörner, Michael Parker, David Bonsall, and Christophe Fraser, *Quantifying SARS-CoV-2 transmission suggests epidemic control with digital contact tracing*, Science **368** (2020), no. 6491, eabb6936.
- [15] Seth Flaxman, Swapnil Mishra, Axel Gandy, H. Juliette T. Unwin, Thomas A. Mclan, Helen Coupland, Charles Whittaker, Harrison Zhu, Tresnia Berah, Jeffrey W. Eaton, Mélodie Monod, Imperial College COVID-19 Response Team, Pablo N. Perez-Guzman, Nora Schmit, Lucia Cilloni, Kylie E. C. Ainslie, Marc Baguelin, Adhiratha Boonyasiri, Olivia Boyd, Lorenzo Cattarino, Laura V. Cooper, Zulma Cucunubá, Gina Cuomo-Dannenburg, Amy Dighe, Bimandra Djaafara, Ilaria Dorigatti, Sabine L. van Elsland, Richard G. FitzJohn, Katy A. M. Gaythorpe, Lily Geidelberg, Nicholas C. Grassly, William D. Green, Timothy Hallett, Arran Hamlet, Wes Hinsley, Ben Jeffrey, Edward Knock, Daniel J. Laydon, Gemma Nedjati-Gilani, Pierre Nouvellet, Kris V. Parag, Igor Siveroni, Hayley A. Thompson, Robert Verity, Erik Volz, Caroline E. Walters, Haowei Wang, Yuanrong Wang, Oliver J. Watson, Peter Winskill, Xiaoyue Xi, Patrick G. T. Walker, Azra C. Ghani, Christl A. Donnelly, Steven Riley, Michaela A. C. Vollmer, Neil M. Ferguson, Lucy C. Okell, and Samir Bhatt, *Estimating the effects of non-pharmaceutical interventions on COVID-19 in Europe*, Nature **584** (2020), no. 7820, 257–261.
- [16] Christophe Fraser, Steven Riley, Roy M. Anderson, and Neil M. Ferguson, *Factors that make an infectious disease outbreak controllable*, Proceedings of the National Academy of Sciences **101** (2004), no. 16, 6146–6151.
- [17] D Klinkenberg, KY Leung, and J Wallinga, *Coronamelder – modelstudie naar effectiviteit. digitaal contactonderzoek in de bestrijding van covid-19*, Rijksinstituut voor Volksgezondheid en Milieu RIVM, 2021.
- [18] Mirjam E. Kretzschmar, Ganna Rozhnova, and Michiel van Boven, *Isolation and contact tracing can tip the scale to containment of COVID-19 in populations with social distancing*, Infectious Diseases (except HIV/AIDS), 2020.
- [19] Adam J Kucharski, Petra Klepac, Andrew J K Conlan, Stephen M Kissler, Maria L Tang, Hannah Fry, Julia R Gog, W John Edmunds, Jon C Emery, Graham Medley, James D Munday, Timothy W Russell, Quentin J Leclerc, Charlie Diamond, Simon R Procter, Amy Gimma, Fiona Yueqian Sun, Hamish P Gibbs, Alicia Rosello, Kevin van Zandvoort, Stéphane Hué, Sophie R Meakin, Arminder K Deol, Gwen

- Knight, Thibaut Jombart, Anna M Foss, Nikos I Bosse, Katherine E Atkins, Billy J Quilty, Rachel Lowe, Kiesha Prem, Stefan Flasche, Carl A B Pearson, Rein M G J Houben, Emily S Nightingale, Akira Endo, Damien C Tully, Yang Liu, Julian Villabona-Arenas, Kathleen O'Reilly, Sebastian Funk, Rosalind M Eggo, Mark Jit, Eleanor M Rees, Joel Hellewell, Samuel Clifford, Christopher I Jarvis, Sam Abbott, Megan Auzenbergs, Nicholas G Davies, and David Simons, *Effectiveness of isolation, testing, contact tracing, and physical distancing on reducing transmission of SARS-CoV-2 in different settings: a mathematical modelling study*, The Lancet Infectious Diseases **20** (2020), no. 10, 1151–1160.
- [20] Fengchen Liu, Wayne T A Enanoria, Jennifer Zipprich, Seth Blumberg, Kathleen Harriman, Sarah F Ackley, William D Wheaton, Justine L Allpress, and Travis C Porco, *The role of vaccination coverage, individual behaviors, and the public health response in the control of measles epidemics: an agent-based simulation for California*, BMC Public Health **15** (2015), no. 1, 447.
- [21] James O. Lloyd-Smith, Alison P. Galvani, and Wayne M. Getz, *Curtailing transmission of severe acute respiratory syndrome within a community and its hospital*, Proceedings of the Royal Society of London. Series B: Biological Sciences **270** (2003), no. 1528, 1979–1989.
- [22] Ira M. Longini, Azhar Nizam, Shufu Xu, Kumnuan Ungchusak, Wanna Hanshaowarakul, Derek A. T. Cummings, and M. Elizabeth Halloran, *Containing Pandemic Influenza at the Source*, Science **309** (2005), no. 5737, 1083–1087.
- [23] Johannes Müller, Mirjam Kretzschmar, and Klaus Dietz, *Contact tracing in stochastic and deterministic epidemic models*, Mathematical Biosciences **164** (2000), no. 1, 39–64.
- [24] Tina R Pollmann, Julia Pollmann, Christoph Wiesinger, Christian Haack, Lolian Shtembari, Andrea Turcati, Birgit Neumair, Stephan Meighen-Berger, Giovanni Zattera, Matthias Neumair, Uljana Apel, Augustine Okolie, Johannes Müller, Stefan Schönert, and Elisa Resconi, *The impact of digital contact tracing on the SARS-CoV-2 pandemic - a comprehensive modelling study*, Public and Global Health, 2020.
- [25] Abbas K. Rizzi, Ali Faqeeh, Arash Badie-Modiri, and Mikko Kivelä, *Epidemic spreading and digital contact tracing: Effects of heterogeneous mixing and quarantine failures*, Phys. Rev. E **105** (2022), 044313.
- [26] Krista C. Swanson, Chiara Altare, Chea Sanford Wesseh, Tolbert Nyenswah, Tashrik Ahmed, Nir Eyal, Esther L. Hamblion, Justin Lessler, David H. Peters, Mathias Altmann, and et al., *Contact tracing performance during the ebola epidemic in liberia, 2014-2015*, PLOS Neglected Tropical Diseases **12** (2018), no. 9.
- [27] Chris Wymant, Luca Ferretti, Daphne Tsallis, Marcos Charalambides, Lucie Abeler-Dörner, David Bonsall, Robert Hinch, Michelle Kendall, Luke Milsom, Matthew Ayres, Chris Holmes, Mark Briers, and Christophe Fraser, *The epidemiological impact of the NHS COVID-19 app*, Nature **594** (2021), no. 7863, 408–412.
- [28] Dongni Zhang and Tom Britton, *Analysing the Effect of Test-and-Trace Strategy in an SIR Epidemic Model*, Bulletin of Mathematical Biology **84** (August 2022), no. 10, 105.